2018

AAVrh10 gene therapy ameliorates central and peripheral nervous system disease in canine globoid cell leukodystrophy (Krabbe disease)

Xuntain Jiang
Washington University School of Medicine in St. Louis

Daniel S. Ory
Washington University School of Medicine in St. Louis

et al

AAVrh10 Gene Therapy Ameliorates Central and Peripheral Nervous System Disease in Canine Globoid Cell Leukodystrophy (Krabbe Disease)

Allison M. Bradbury,[1,*] Mohammed A. Rafi,[2] Jessica H. Bagel,[1] Becky K. Brisson,[1] Michael S. Marshall,[3] Jill Pesayco Salvador,[4] Xuntain Jiang,[5] Gary P. Swain,[1] Maria L. Prociuk,[1] Patricia A. ODonnell,[1] Caitlin Fitzgerald,[1] Daniel S. Ory,[5] Ernesto R. Bongarzone,[3,6] G. Diane Shelton,[4] David A. Wenger,[2] and Charles H. Vite[1]

[1]Department of Clinical Sciences and Advanced Medicine, School of Veterinary Medicine, University of Pennsylvania, Philadelphia, Pennsylvania; [2]Department of Neurology, Sidney Kimmel College of Medicine, Thomas Jefferson University, Philadelphia, Pennsylvania; [3]Department of Anatomy and Cell Biology, College of Medicine, University of Illinois, Chicago, Illinois; [4]Department of Pathology, School of Medicine, Comparative Neuromuscular Laboratory, University of California, San Diego, La Jolla, California; [5]Diabetic Cardiovascular Disease Center, Washington University School of Medicine, St. Louis, Missouri; [6]Departamento de Química Biologica, Facultad de Farmacia y Bioquímica, Universidad de Buenos Aires, Argentina.

Globoid cell leukodystrophy (GLD), or Krabbe disease, is an inherited, neurologic disorder that results from deficiency of a lysosomal enzyme, galactosylceramidase. Most commonly, deficits of galactosylceramidase result in widespread central and peripheral nervous system demyelination and death in affected infants typically by 2 years of age. Hematopoietic stem-cell transplantation is the current standard of care in children diagnosed prior to symptom onset. However, disease correction is incomplete. Herein, the first adeno-associated virus (AAV) gene therapy experiments are presented in a naturally occurring canine model of GLD that closely recapitulates the clinical disease progression, neuropathological alterations, and biochemical abnormalities observed in human patients. Adapted from studies in twitcher mice, GLD dogs were treated by combination intravenous and intracerebroventricular injections of AAVrh10 to target both the peripheral and central nervous systems. Combination of intravenous and intracerebroventricular AAV gene therapy had a clear dose response and resulted in delayed onset of clinical signs, extended life-span, correction of biochemical defects, and attenuation of neuropathology. For the first time, therapeutic effect has been established in the canine model of GLD by targeting both peripheral and central nervous system impairments with potential clinical implications for GLD patients.

Keywords: globoid cell leukodystrophy (Krabbe disease), canine model, AAV gene therapy, neurodegenerative disease, lysosomal storage disorder, leukodystrophy

INTRODUCTION

GLOBOID CELL LEUKODYSTROPHY (GLD), also known as Krabbe disease, is a genetic, currently incurable, neurodegenerative disease caused by a defect in the gene encoding the hydrolytic enzyme galactosylceramidase (GALC), which is responsible for the lysosomal degradation of important myelin lipids, including galactosylceramides. The deficiency in GALC activity also results in the accumulation of galactosylsphingosine (psychosine) to levels that become toxic to oligodendrocytes and Schwann cells, and causes diffuse central nervous system (CNS) and peripheral nervous system (PNS) demyelination. The prevalence of GLD in families with European ancestry is estimated to be about 1:100,000 live births in the United States. Most individuals with GLD present as infants or in early childhood with clinical signs of irritability, stiffness, loss of developmental milestones, and seizures, with disease progressing to the loss of most bodily functions, a vegetative state, and early childhood death.[1,2]

To date, the only available therapy for children with GLD is hematopoietic stem-cell transplanta-

*Correspondence: Dr. Allison M. Bradbury, University of Pennsylvania, School of Veterinary Medicine, 3800 Spruce Street, 208 Rosenthal Building, Philadelphia, PA 19104. E-mail: brada@upenn.edu

DOI: 10.1089/hum.2017.151

tion (HSCT) from donor umbilical cord blood or bone marrow. When infants are transplanted presymptomatically, children initially show a slowing of the disease progression.[3] However, when followed long term, 20% of transplanted children have near normal function, 40% walk with assisted devices, and the remaining 40% are severely impaired and wheelchair-bound.[4] Continued disease progression following HSCT is likely due to insufficient GALC activity in the CNS and/or insufficient treatment of the PNS.

Experimental therapies have been extensively evaluated in the naturally occurring murine model of GLD, the twitcher mouse. HSCT from enzymatically normal donor mice into twitcher mice resulted in a moderate but significant increase in life-span from about 40 days in untreated affected mice to a mean of 80 days in transplanted mice.[5–10] With the advent of safer and more efficient viral vehicles, adeno-associated virus (AAV) gene therapy has also been comprehensively evaluated in twitcher mice over the last decade. Bilateral intracerebroventricular (ICV) injections of AAV serotype 1 encoding murine *GALC* (AAV1-mGALC) into neonatal twitcher mice increased life-span to a median of $\sim$56 days (66 days maximum).[11] AAV serotype 5 encoding murine *GALC* (AAV5-mGALC) delivered by intracranial (IC) injection extended life-span to an average of 63 days (66 days maximum),[12] and IC plus intrathecal injection to a median life-span of 71 days (78 days maximum).[13] Intravenous (i.v.) delivery of AAV serotype rh10 encoding murine *GALC* (AAVrh10-mGALC) on postnatal day 2 resulted in an average life-span of 55 days (63 days maximum), while mice treated with ICV and intra-cerebellar injections lived an average of 81 days (140 days maximum).[14] Importantly, combination of both i.v. and CNS-directed gene therapy (ICV and intra-cerebellar) had a synergistic effect and resulted in an average life-span of 104 days, with several mice living up to 150 days. A second i.v. injection 5 days after the initial dose further extended life-span to an average of 120 days.[14] The dramatic improvements in behavior, life-span, CNS GALC enzyme activity, and CNS and PNS pathology warranted evaluation of combination i.v. and ICV AAV gene therapy in a large-animal model of GLD.

GLD is a hereditary disease in dogs, and disease progression closely recapitulates human disease.[15–17] Dogs are the only naturally occurring disease model that results from a missense mutation, c.473A>C, p.158Y>S, in the *GALC* gene, which is inherited as an autosomal recessive trait.[16] Transient transfection of COS-1 cells with the mutant canine *GALC cDNA* results in no GALC activity in transfected cells,[16] indicating that mutant protein is not functional. Signs in affected dogs begin at $\sim$6 weeks of age with pelvic limb weakness, thoracic limb dysmetria, and head tremor. Disease then progresses to include ataxia, pelvic limb paresis, urinary incontinence, and loss of hearing by 12 weeks of age. Pelvic limb paralysis warrants euthanasia at a mean $\pm$ *SD* of 15.7 $\pm$ 4.8 weeks of age (n = 19).[18] Magnetic resonance imaging (MRI) of the brains of GLD dogs demonstrates changes consistent with demyelination,[19] and magnetic resonance spectroscopy confirms decreases in N-acetylaspartate and increases in choline, indicative of neuronal loss and abnormal myelin turnover, respectively.[20] Diffusion tensor imaging of the canine GLD brain shows substantial decreases in fractional anisotropy, increases in radial diffusivity, and increases in apparent diffusion coefficient in the internal capsule, corona radiata, and corpus callosum when compared to normal dogs.[21] Consistent with imaging findings, histologic evaluation shows severe loss of myelin and globoid cell accumulation in white matter.[18] Brain biochemistry reveals decreased GALC activity and elevated psychosine levels.[15]

Herein, the first AAV gene therapy experiments in a large-animal model of GLD are presented. Adapted from studies in twitcher mice,[14] GLD-affected dogs were treated by AAVrh10 vectors encoding either a reporter protein or therapeutic *GALC* transgene by combination i.v. and ICV injections to evaluate the effect on both PNS and CNS disease. For the first time, biodistribution studies with a reporter protein delivered by combination i.v. + ICV routes in a large animal are demonstrated. More importantly, a therapeutic effect in the canine model of GLD is also established, with marked improvement seen in PNS function and histology.

MATERIALS AND METHODS

Animals and AAV vector injections

Dogs were raised in the National Referral Center for Animal Models of Human Genetic Disease of the School of Veterinary Medicine of the University of Pennsylvania (NIH OD P40-10939) under National Institutes of Health and USDA guidelines for the care and use of animals in research. The experimental protocol was approved by the university's Institutional Animal Care and Use Committee. GLD in dogs is due to a missense mutation *GALC* gene, c.473A>C, p.158Y>S. Whole blood from dogs was tested for the *GALC* missense mu-

tation using TaqMan® real-time polymerase chain reaction (PCR)-based DNA test to identify affected, normal, and heterozygote dogs. The custom TaqMan® SNP genotyping assay included forward primer: ACTGGCCTTACGTGAATCTTCAG, and reverse primer: GCTTGGCACCCACAATCC, with VIC/NFQ as the reporter/quencher for allele 1 and FAM/NFQ for allele 2. Using a TaqMan® Genotyping Master Mix (#4371353, Life Technologies, Grand Island, NY), the assay was run on an Applied Biosystems 7500 platform (Applied Biosystems, Foster City, CA).

Two GLD dogs were treated with AAVrh10 expressing green florescent protein (GFP; AAVrh10-GFP), one dog by i.v. injection alone and the second dog by i.v. and ICV injection, at a dose of 4.3E12 vector genomes (vg; Table 1). All subsequent dogs received i.v. and ICV injections. One GLD dog was treated with AAVrh10 encoding the human *GALC* transgene (AAVrh10-hGALC) at a total dose of 3.5E12 vg (Table 1). Two GLD dogs received AAVrh10-cGALC at a total dose of 1.2E12 vg (Table 1; referred to as low dose), and two additional GLD dogs were treated with an increased dose of AAVrh10-cGALC, 3.8E13 vg (Table 1; referred to as high dose). For i.v. injection of GLD dogs at 3 days of age, the skin was clipped and scrubbed with 4% chlorohex followed by 70% isopropyl alcohol. A catheter was placed in the jugular vein. Saline was injected to clear the line, then 500 μL of AAVrh10-GFP, 500 μL of AAVrh10-hGALC, 500 μL of low-dose AAVrh10-cGALC, or 1,000 μL of high-dose AAVrh10-cGALC was injected over <1 min, saline was injected to clear the line, and the catheter removed. For ICV injections at 6 weeks of age, prior to onset of neurological dysfunction, GLD dogs were anesthetized with propofol, intubated, maintained on isoflurane, and placed in a Kopf stereotaxic head holder, and the head was clipped and scrubbed for aseptic surgery. A 2-cm-long skin incision was made in the dorsal midline of the skin over the skull, and subcutaneous tissue was moved aside. A 25G drill bit was used to drill a hole in the left side of the skull at the following position: 0.5 cm lateral and 1.0 cm caudal to the bregma. A 1.0 mL syringe with a 1.5″ 22G needle was inserted into the brain with 0.1 mL of suction until cerebrospinal fluid (CSF) was seen in the hub. The depth was recorded, and the needle removed. A 1.0 mL syringe with a 1.5″ 22G needle filled with 500 μL of AAVrh10-GFP, 1,000 μL of AAVrh10-hGALC, 500 μL of low-dose AAVrh10-cGALC, or 1,000 μL of high-dose AAVrh10-cGALC was inserted into the brain and advanced to the depth determined by the first needle ($\sim$1–2 cm). Vector was injected into the left lateral ventricle, and the needle was withdrawn. A nylon skin suture was placed, and the dog was recovered. After all procedures, animals were closely monitored. Untreated and treated GLD dogs were euthanized at a humane endpoint defined by complete pelvic limb paralysis. Euthanasia was performed using an overdose of i.v. barbiturate. After sacrifice, animals were perfused through the left ventricle with 750 mL of 0.9% cold saline, and tissues were collected.

Table 1. *Treatment cohorts and survival*

	Treatment	*Injection route*	*Dose (vg)*	*Survival (weeks)*
1	AAVrh10-GFP	i.v. (3 days)	4.3E12	17.4
2				11.3
3	AAVrh10-hGALC		3.5E12	9.1
4	AAVrh10-cGALC	i.v. (3 days) + ICV (6 weeks)	1.2E12 (low)	22.1
5				17.9
6			3.8E13 (high)	30.3
7				43.1

vg, vector genomes; i.v., intravenous; ICV, intracerebroventricular.

Vector production

GFP, human *GALC*, or canine *GALC* cDNA was cloned into EcoRI site of a CB7 plasmid, downstream from the human CMV-enhancer/chicken β-actin hybrid promoter. The accuracy of the transgene was confirmed by sequencing, the integrity of the 5′and 3′ inverted terminal repeats (ITRs) was confirmed by restriction enzyme analysis, and the functionality of the construct was verified by *in vitro* cell transfection and measurement of GALC enzyme activity. The plasmid was cross-packaged by the Institute of Human Gene Therapy at the University of Pennsylvania into AAVrh10,[22] and large-scale vector preparations were generated, as previously described.[23]

Nerve conduction velocity

Dogs were anesthetized with propofol, endotracheally intubated, and maintained on isoflurane anesthesia. Nerve conduction velocity (NCV) was quantified using an electrodiagnostics machine (Nicolet Viking Quest; Nicolet Biomedical, Madison, WI). Motor NCV in the tibial, sciatic, and ulnar nerves of the left limb was determined using 12 mm, 29G subdermal needle recording electrodes placed in the interosseous muscle. The tibial nerve was electrically stimulated at the tarsus. The sciatic nerve was electrically stimulated at the stifle and at the level of the femoral head. The ulnar nerve was stimulated at the carpus and elbow. Nerves were stimulated with monopolar stimulating electrodes placed subcutaneously for a duration

of 200 μs. Stimulus intensity was increased until a M wave of maximal amplitude was obtained. Sensory NCV was determined for the radial nerve. Subcutaneous recording electrodes were placed lateral to the radial nerve at the level of the elbow and the skin over the dorsum of the paw and stimulated with subcutaneous monopolar stimulating electrodes for 200 μs.

Brain-stem auditory evoked response

Dogs were anesthetized with propofol, endotracheally intubated, and maintained on isoflurane anesthesia. Brain-stem auditory evoked response (BAER) data were recorded on a Nicolet Viking Quest machine (Nicolet Biomedical) using 12 mm, 29G subdermal needle recording electrodes. The active electrode was placed in the skin over the osseous bulla of the stimulated ear, the reference electrode in the skin over the vertex of the skull, and the ground electrode in the skin over the contralateral osseous bulla. Alternating rarefaction and condensation clicks (0.1 ms duration) were delivered to the stimulated ear at 11.1 Hz using a 25 cm plastic tube connected to a plastic ear piece placed within the external ear canal. The filter settings for the amplifier were set to 20 Hz and 3 kHz. One thousand evoked responses were averaged for each tracing obtained. An amplifier sensitivity of 1 μV/cm was used to record the responses; the analysis time was 10 ms. Central conduction time was defined as the time between the first and the fifth peak. Hearing threshold was defined as the sound intensity at which an evoked waveform was first visible.

Quantification of GALC enzyme activity

Tissue homogenates (20 μg) in pure H_2O were incubated with fluorescent GALC substrate (6HMU-beta-D-galactoside; Moscerdam Substrates, Oegstgeest, The Netherlands) for 17 h at 37°C. Enzymatic activity was assessed via fluorescence, as measured with a Beckmann Coulter DTX 880 multimode detector using excitation/emission wavelengths of 385 nm and 450 nm, respectively.

Quantification of tissue psychosine

Psychosine from tissue homogenates (200 μg) was extracted via a methanol–acetic acid solution. Analysis was then performed on a Shimadzu (Kyoto, Japan) Nexera UHPLC system equipped with a Waters Acquity UPLC BEH amide column and coupled to a Shimadzu LCMS-8050 triple quadrupole mass spectrometer equipped with positive ion electrospray. D-lactosyl-β1-1′-D-*erythro*-sphingosine (Avanti Polar Lipids, Alabaster, AL) was used as an internal standard.

Quantification of CSF psychosine

Protein precipitation was performed to extract psychosine from 50 μL of dog CSF. Deuterated galactosyl sphingosine (psychosine d_5: 1 ng/mL) was used as an internal standard and was added to the samples before extraction. Quality control (QC) samples were prepared by pooling the extracts from study samples. QC was run on every five-study samples to make sure that the analytical method and instrument response was constant. Sample analysis was performed with a Shimadzu 20AD HPLC system, coupled to a triple quadrupole mass spectrometer (API 4000 QTrap; Sciex, Framingham, MA) operated in MRM mode. The positive ion ESI mode was used for detection of psychosine and deuterated psychosine–d_5. Data processing was conducted with Analyst 1.5.1 (Applied Biosystems).

Vector quantification

Samples were stored at –80°C until the time of analysis. Total cellular DNA was extracted from tissue using a QIAamp DNA Mini Kit (Qiagen, Valencia, CA). Detection and quantification of vg in extracted DNA were performed by real-time PCR (TaqMan® Universal Master Mix; Applied Biosystems) using a primer and FAM-TAMRA probe set targeted to polyA adenylation signal in the vector. The PCR conditions were: 100 ng total cellular DNA as template, 300 nM primers, and 200 nM probe per reaction. Cycles were: 10 min at 95°C, 40 cycles of 15 s at 95°C, and 1 min at 60°C. Results were compared to a standard curve of known copy numbers generated from the plasmid used to make vector.

Neutralizing antibody assay

Neutralizing antibody titers to AAVrh10 were conducted at the Immunology Core in the Department of Pathology and Laboratory Medicine at the University of Pennsylvania. The assay was conducted as previously described,[24] with the exception of an initial dilution of 1:5 and use of HEK293 cell line.

Histology

Perfused brains were fixed in 4% paraformaldehyde, and paraffin embedded. Sections were cut at 5 μ, and slides were deparaffinized and rehydrated in a series of xylenes and ethanols (100%, 95%, 70%). For myelin staining, slides were incubated in an eriochrome cyanine R solution (#32752; Sigma–Aldrich, St. Louis, MO) with ferric chloride and sulfuric acid for 30 min at room temperature, rinsed in running water, and incubated in an iron (III) nitrate nonahydrate (#216828; Sigma–Aldrich) differentiating solution for 2–5 min and rinsed in

running water. Slides were counterstained with eosin and dehydrated in a series of ethanols and xylenes and mounted. For periodic acid–Schiff (PAS) staining, slides were incubated in periodic acid solution (#3951; Sigma–Aldrich) for 5 min at room temperature, rinsed with several changes of water, followed by incubation in Schiff's reagent (#3952016; Sigma–Aldrich) for 15 min. Slides were rinsed in running water, dehydrated in a series of ethanols and xylenes, and mounted. For immunofluorescence, deparaffinized and rehydrated slides were heated to a boil followed by a 30 min incubation in antigen retrieval solution (#HK086; Biogenex, Fremont, CA). Primary antibodies were diluted in antibody diluent reagent solution (#003118; Life Technologies, Waltham, MA) as follows: rabbit polyclonal ionized calcium-binding adapter molecule 1 (Iba1) (#CP290; Biocare, Concord, CA) 1:100; mouse monoclonal glial fibrillary acidic protein (GFAP; #556329; BD Pharmingen, San Jose, CA) 1:100; mouse monoclonal lysosomal-associated membrane protein 1 (LAMP1; #B10407; LifeSpan BioSciences, Seattle, WA) 1:750. They were then incubated covered at 37°C for 1 h. Following three 5 min washes with phosphate-buffered saline (PBS), goat anti-mouse 488-conjugated (#A-11029; Thermo Fisher Scientific, Waltham, MA) and goat anti-rabbit 568-conjugated (#A-11036; Thermo Fisher Scientific) secondary antibodies were applied at a dilution of 1:500 in antibody diluent reagent solution. Following three 5 min washes with PBS, slides were stained with DAPI for 1 min and mounted.

Peripheral nerve analysis: light microscopy and morphometry

Peripheral nerve specimens were collected from the sciatic, tibial, and superficial radial nerves immediately following euthanasia and saline perfusion. Specimens were either immersion-fixed into 10% neutral-buffered formalin or wrapped in a saline dampened gauze sponge, placed into a watertight container, and chilled during transport. Upon receipt, fixed nerves were transferred to 2.5% glutaraldehyde, post-fixed in 1% aqueous osmium tetroxide, and processed to araldite resin blocks. Sections (1 μm thick) were cut and stained with toluidine blue and paraphenelenediamine prior to light microscopic examination. Frozen sections of each nerve were stained with modified Gomori trichrome stain to localize myelin or reacted with acid phosphatase to localize lipid-containing macrophages (globoid cells).

For quantitative assessment, high-quality nerve specimens adequately fixed and free of artifact were chosen. Using point counting techniques and a grid with a magnified distance of 0.08 mm between intersection points, the fascicular area, defined as the number of points falling on the endoneurium of nerve fascicles, was determined. The total number of myelinated fibers, the number of fibers with inappropriately thin myelin sheaths relative to their axon diameter, as well as those with myelin splitting and ballooning, and the number of probable regenerative clusters (defined as two or more closely apposed myelinated fibers) were assessed in each nerve specimen and normalized to the fascicular area. As previously described,[25,26] only those fibers with clear, faintly staining space evident between separated myelin with an asymmetrical profile were considered to have splitting and ballooning, while profiles containing paranodal regions or Schmidt–Lanterman clefts were not counted. In addition, computer-assisted analyses of axonal size–frequency distributions of myelinated fibers, nerve fiber diameter, axonal diameter, myelin thickness, and G ratio (structural index of axonal myelination defined as axonal diameter/fiber diameter based on measurements by perimeter) were determined using SPOT™ Advanced Imaging software and modifications of Adobe Photoshop.

Statistics

Two-tailed, unpaired *t*-tests and figures were conducted using Graph Pad Prism v6 (GraphPad Software, La Jolla, CA). Levels of significance were set at *p*-values of ≤0.05, ≤0.01, and ≤0.001.

RESULTS

Treatment cohorts and survival

Two GLD dogs received AAVrh10-GFP by either i.v. injection alone or by a combination of i.v. and ICV injections routes (Table 1). Intravenous injections were conducted at 3 days of age, once genotype was confirmed, and ICV injections were done at 6 weeks of age, when dogs can safely undergo general anesthesia and surgery. The two dogs were euthanized at 11.3 and 17.4 weeks of age due to signs of progressive GLD-related disease. This survival time is comparable to the mean life-span of untreated GLD dogs ($M \pm SD = 15.7 \pm 4.8$ weeks; $n = 19$).

Five GLD dogs received AAVrh10 encoding the therapeutic *GALC* transgene by a combination of i.v. and ICV routes at 3 days and 6 weeks of age, respectively. One GLD dog was treated with AAVrh10 encoding the human *GALC* transgene (AAVrh10-hGALC) at a dose of 3.5E12 vg and died at 9.1 weeks of age (Table 1). Due to the potential for immunogenicity of the human transgene, the

canine *GALC* cDNA was packaged into the same AAVrh10 backbone (AAVrh10-cGALC). Two GLD dogs received AAVrh10-cGALC at a dose of 1.2E12 vg (Table 1; referred to as low dose), divided evenly between i.v. and ICV injection routes. These dogs were euthanized at 17.9 and 22.1 weeks of age due to signs of progressive GLD-related disease. Two additional GLD dogs were treated with an increased dose of AAVrh10-cGALC, 3.8E13 vg (Table 1; referred to as high dose), again divided evenly between i.v. and ICV injection routes. Survival of high-dose-treated dogs was increased to 30.3 and 43.1 weeks of age, when the dogs were euthanized due to signs of progressive GLD-related disease (Table 1).

Clinical evaluation of AAVrh10-treated dogs

Untreated GLD dogs show no neurological deficits until approximately 6 weeks of age. The earliest signs of disease include tremors and ataxia. Severity of tremors and ataxia increase over time, and pelvic limb paralysis, the defined humane endpoint, develops by 15.7 ± 4.8 weeks age[18] (Supplementary Video S1; untreated GLD dog at 14 weeks of age; Supplementary Data are available online at www.liebertpub.com/hum). Administration of AAVrh10-GFP had no effect on the onset or progression of clinical signs or life-span (Supplementary Video S1; AAVrh10-GFP-treated dog at 15 weeks of age). In contrast, a littermate GLD dog treated with low-dose AAVrh10 encoding canine *GALC* had only mild signs of neurologic disease at 15 weeks of age (Supplementary Video S1; AAVrh10-cGALC low-dose-treated dog at 15 weeks of age). Although both GLD dogs that received low-dose AAVrh10-cGALC showed improved ambulation at 15 weeks of age compared to untreated dogs, both dogs were euthanized due to pelvic limb paralysis at ages comparable to that of untreated GLD dogs.

In contrast, dogs that received high-dose AAVrh10-cGALC showed a greater delay in the onset and progression of clinical signs and lived longer. At 34 weeks of age, one dog treated with the high-dose combination therapy had mild ataxia and no evidence of tremor (Supplementary Video S2; AAVrh10-cGALC high-dose-treated dog at 34 weeks of age). This dog only became paralyzed at 43 weeks of age. The other dog from the high-dose cohort progressed slightly more rapidly, as it had moderate ataxia, resulting in repeated falling when walking at 26 weeks of age, and became paralyzed at 30 weeks of age. This dog also remained without tremor at the defined endpoint. Although progression was slowed in both dogs, each dog eventually progressed to pelvic limb paralysis, the defined humane endpoint.

A single dog that was administered AAVrh10-hGALC died suddenly at 9.1 weeks of age. At the time of death, the dog showed tremor, pelvic limb paresis, and spinal ataxia comparable to that of untreated GLD dogs; pelvic limb paralysis was not present. The cause of the sudden death was not determined. However, clinical signs at the time of death were consistent with near end-stage GLD disease.

Peripheral NCV and BAER testing were performed on untreated GLD dogs at the defined endpoint (14–19 weeks of age; $n = 6$), normal age-matched control dogs (14–21 weeks; $n = 9$), and AAVrh10-treated GLD dogs at the defined endpoint. Motor NCVs were significantly decreased in untreated GLD dogs, indicative of demyelination, when compared to age-matched normal control dogs for the tibial (Fig. 1A; $p = 0.0093$), sciatic (Fig. 1B; $p = 0.0021$), and ulnar nerves (Fig. 1C; $p = 0.0134$). Sensory NCV of the superficial radial nerve was also significantly reduced (Fig. 1D; $p = 0.0033$) in untreated GLD dogs when compared to normal control dogs. As expected, i.v. and ICV delivery of AAVrh10 encoding the reporter *GFP* transgene had no effect on motor or sensory NCV. AAVrh10 encoding canine *GALC* at a low dose had a modest effect on NCVs (Fig. 1A–D). However, use of high-dose AAVrh10-cGALC normalized NCV for motor measurements (Fig. 1A–C) and nearly normalized sensory NCV (Fig. 1D).

BAER testing demonstrated a significant increase in central conduction time (data not shown) and hearing threshold in the left (Supplementary Fig. S1A; $p = 0.0001$) and right (Supplementary Fig. S1B; $p = 0.0015$) ears of untreated GLD dogs when compared to normal dogs. AAV-mediated transfer of either transgene (*GFP* or canine *GALC*) or dose (cGALC low or high) had a negligible effect, as treated animals showed no improvement in central conduction time (data not shown) or hearing threshold over untreated animals (Supplementary Fig. S1A and B).

GALC and psychosine quantification in AAVrh10-cGALC-treated GLD dogs

GALC activity and psychosine concentration were measured in the cerebellum, cerebrum, lumbar spinal cord, sciatic nerve, and liver of normal, GLD, and AAVrh10-cGALC-treated dogs (Table 2). GALC activity was greatly reduced in the cerebellum of untreated GLD dogs to 0.04 pmol/h/μg protein ($SD = 0.04$; $n = 6$), with many dogs below the level of detection, when compared to normal (0.31 ± 0.07 pmol/h/μg protein; $n = 5$). Correspondingly, psychosine concentrations in this brain re-

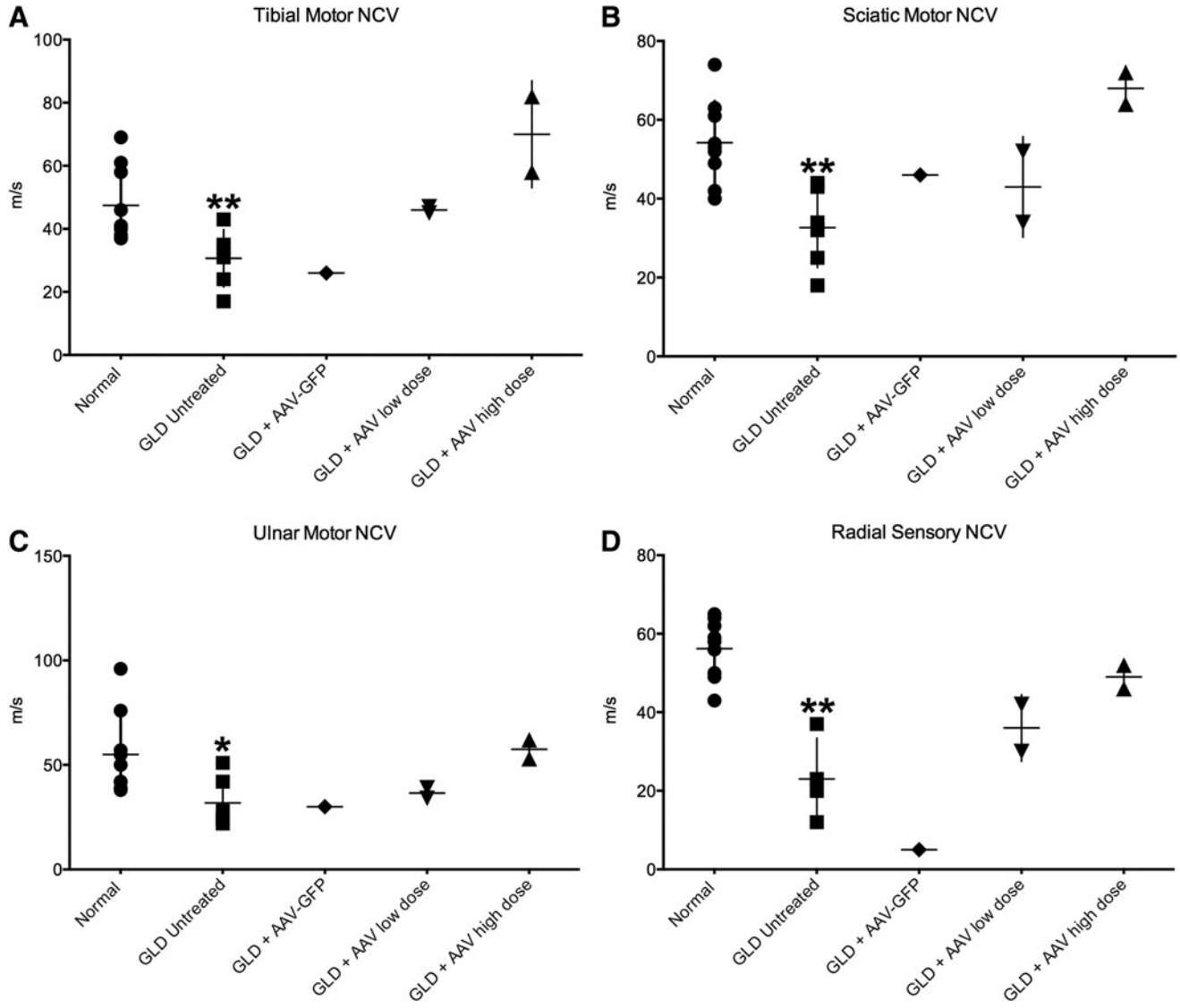

Figure 1. Nerve conduction velocity (NCV) in normal, globoid cell leukodystrophy (GLD), and adeno-associated virus (AAV)-treated dogs. NCV was conducted on untreated GLD dogs at the defined humane endpoint (14–19 weeks of age; $n=6$; *solid square*), normal age-matched control dogs (14–21 weeks; $n=9$; *solid circle*), and AAV-treated GLD dogs at endpoint (AAV-GFP, $n=1$, *solid diamond*; AAVrh10-cGALC low dose, $n=2$, *solid triangle*; AAVrh10-cGALC high dose, $n=2$, *solid triangle*). For pelvic limb motor NCV, the **(A)** tibial nerve was stimulated at the tarsus and stifle, the **(B)** sciatic nerve was stimulated at the stifle and at the level of the femoral head, and for the thoracic limb the **(C)** ulnar nerve was stimulated at the carpus and elbow, and for sensory NCV the **(D)** radial nerve at the level of the elbow. *$p \leq 0.05$; **$p \leq 0.01$.

gion were increased 10-fold over normal, with an average of 218.52 pmol/mg protein compared to normal levels of 22.91 pmol/mg protein ($SD=15.90$; $n=5$). However, values were variable within the untreated GLD cohort, with a range of 45.34–748.39 ($n=6$). One GLD dog treated with high-dose AAVrh10-cGALC achieved normal GALC activity in the cerebellum (0.56 pmol/h/μg protein). However, cerebellar psychosine remained elevated at 159.47 pmol/mg protein. The longer-living dog from the high-dose cohort had supraphysiologic levels of GALC in the cerebellum at 2.41 pmol/h/μg protein, and had psychosine concentrations within the normal range (28.15 pmol/mg protein). GALC activities in the cerebrum of normal (0.36 ± 0.10 pmol/h/μg protein) and GLD (0.01 ± 0.00 pmol/h/μg protein) dogs were comparable to those found the cerebellum. However, psychosine levels in the cerebrum of normal (5.25 ± 3.94 pmol/mg protein) and GLD (45.82 ± 29.18 pmol/mg protein) dogs were lower compared to the cerebellum. Both high-dose-treated dogs had increased levels of GALC (0.23 and 0.22 pmol/h/μg protein) in the cerebrum compared to untreated dogs, and the longer-living dog again had a greater reduction of psychosine (21.92 compared to 41.93 pmol/mg protein). In the lumbar

Table 2. *GALC activity, psychosine concentration, and vector copy number*

	Cerebellum			*Cerebrum*			*Spinal Cord*			*Sciatic Nerve*			*Liver*		
	GALC avg. (SD)	*Psy avg. (SD)*	*Vector copy number*	*GALC avg. (SD)*	*Psy avg. (SD)*	*Vector copy number*	*GALC avg. (SD)*	*Psy avg. (SD)*	*Vector copy number*	*GALC avg. (SD)*	*Psy avg. (SD)*	*Vector copy number*	*GALC avg. (SD)*	*Psy avg. (SD)*	*Vector copy number*
Normal	0.31 (0.07)	22.91 (15.90)		0.36 (0.10)	5.25 (3.94)		0.14 (0.01)	22.55 (4.03)		0.05 (0.05)	17.10 (10.73)		0.88 (0.20)	0	
GLD	0.04 (0.04)	218.52 (244.52)	BLD	0.01 (0.00)	45.82 (29.18)	BLD	0.07 (0.03)	307.05 (52.36)	BLD	0.01 (0.00)	355.45 (10.69)	BLD	0.06 (0.02)	3.43 (1.47)	BLD
AAV-cGALC							0	54.72	1.41E + 04	0	238.16	4.45E + 02	0.14	3.66	1.30E + 03
low dose			NA				0	84.69	1.15E + 05	0	202.29	1.96E + 01	0.2	2.68	1.93E + 03
AAV-cGALC	0.56	159.47	1.51E + 05	0.23	41.93	4.06E + 05	0.19	5.514	2.52E + 06	0.48	42.76	4.32E + 05	0.82	0.28	6.02E + 06
high dose	2.41	28.15	1.04E + 06	0.22	21.92	7.10E + 05	0.13	69.71	3.06E + 06	0.07	17.39	3.67E + 05	0.93	0.27	2.65E + 06

GALC is shown as pmol/h/μg protein; Psy is shown as pmol/mg protein; vector copy number is shown per 100 ng of DNA.
GLD, globoid cell leukodystrophy; AAV, adeno-associated virus; GALC, galactosylceramide activity; cGALC, canine GALC; Psy, psychosine concentration; Avg, average; *SD*, standard deviation; BLD, below level of detection; NA, not assayed.

spinal cord, levels of psychosine in untreated GLD dogs (307.05 ± 52.36 pmol/mg protein compared to normal 22.55 ± 4.03 pmol/mg protein) were greater than the cerebellum, despite slightly more GALC activity (0.07 ± 0.03 pmol/h/μg protein). Low-dose-treated dogs had undetectable levels of GALC activity in the lumbar cord. Yet, some reduction in psychosine to 54.72 and 84.69 pmol/mg protein was achieved. High-dose-treated dogs had normalized GALC levels (0.19 and 0.13 pmol/h/μg protein) and variable reduction in psychosine concentration (5.51 and 69.71 pmol/mg protein) in the lumbar cord. In the sciatic nerve, GLD dogs had GALC activity comparable to the brain 0.01 pmol/h/μg protein ($SD = 0.002$), and the highest psychosine levels in all regions tested, averaging 355.45 pmol/mg protein ($SD = 10.69$). Normal dogs had lower GALC activity (0.05 ± 0.05 pmol/h/μg protein) and psychosine (17.10 ± 10.73 pmol/mg protein) in the sciatic nerve than the brain. In the low-dose cohort, dogs had undetectable levels of GALC in the sciatic nerve and only modestly reduced psychosine concentrations to 238.16 and 202.29 pmol/mg protein, while the high-dose-treated dogs had normal or supraphysiological GALC (0.07 and 0.48 pmol/h/μg protein) and greater reductions in psychosine (17.39 and 42.76 pmol/mg protein). In the liver, GALC activity in normal dogs averaged 0.88 pmol/h/μg protein ($SD = 0.20$; $n = 5$), and psychosine was undetectable in all samples. In untreated GLD dogs, GALC activity was reduced to 0.06 pmol/h/μg protein ($SD = 0.02$; $n = 6$), with many dogs below the level of detection. Psychosine concentration in the liver of GLD dogs was elevated to 3.4 pmol/mg protein ($SD = 1.5$; $n = 6$) and was highest in the two oldest dogs evaluated (both >5 pmol/mg protein). Dogs treated with low-dose AAVrh10-cGALC had modestly elevated GALC activities of 0.14 and 0.20 pmol/h/μg protein, and psychosine levels comparable to untreated GLD dogs at 3.7 and 2.7 pmol/mg protein. Dogs treated with high-dose AAVrh10-cGALC had completely normalized levels of GALC in the liver (0.82 and 0.93 pmol/h/μg protein) and considerably reduced psychosine concentration to 0.28 and 0.27 pmol/mg protein (Table 2).

CSF psychosine quantification

Psychosine was quantified in endpoint CSF samples of the four dogs treated with AAVrh10-cGALC, as well as untreated GLD dogs at the endpoint ($n = 5$) and normal age-matched controls ($n = 5$; Fig. 2). It was previously shown that CSF psychosine concentrations were significantly elevated in GLD affected dogs ($p = 0.004$) compared to age-matched normal control dogs, in which

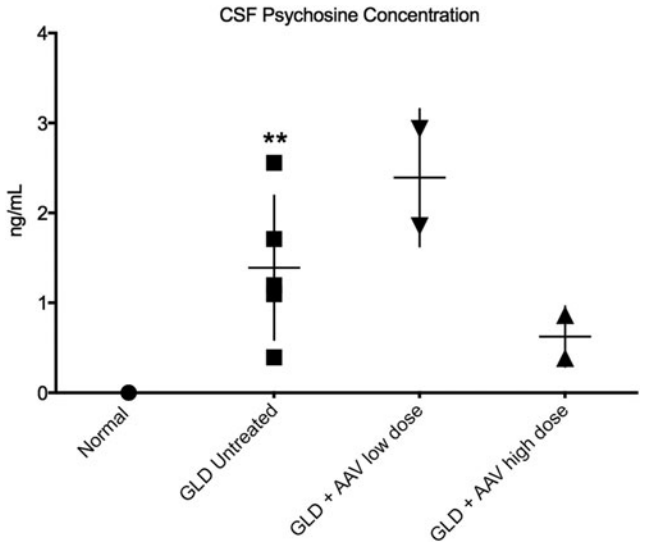

Figure 2. Cerebrospinal fluid (CSF) psychosine concentration in normal, GLD, and AAV-treated dogs. CSF psychosine concentrations determined by high-performance liquid chromatography (HPLC) coupled-mass spectrometry and presented as concentration (ng/mL) for GLD-affected dogs (*solid square*; $n=5$; $M_{age}=13.4$ weeks, range 10.9–16.4 weeks) compared to normal control dogs (*solid circle*; $n=5$; $M_{age}=18.0$ weeks, range 6.1–38.7 weeks) and AAVrh10-treated GLD dogs at endpoint (AAVrh10-cGALC low dose, $n=2$, *solid triangle*; AAVrh10-cGALC high dose, $n=2$, *solid triangle*). $^{**}p \leq 0.01$.

psychosine was undetectable.[18] GLD dogs treated with low-dose AAV had CSF psychosine concentrations (2.39 ± 0.54 ng/mL) similar to untreated GLD dogs. However, GLD dogs treated with high-dose AAV had CSF psychosine concentrations (0.62 ± 0.23 ng/mL) lower than untreated and low-dose AAV-treated GLD dogs, despite being substantially older.

AAV vector quantification

AAVrh10 vector copy numbers were quantified in the cerebellum, cerebrum, lumbar spinal cord, sciatic nerve, and liver by quantitative PCR with primers specific to the polyA adenylation signal of the vector. The high-dose AAVrh10-cGALC-treated dogs had the greatest number of vector copies in the liver (6.02E + 06, 2.65E + 06), spinal cord (2.52E + 06, 3.06E + 06), and cerebellum (1.51E + 05, 1.04E + 06) and slightly reduced numbers in the cerebrum (4.06E + 05, 7.10E + 05) and sciatic nerve (4.32E + 05, 3.67E + 05; Table 2). In all tissues analyzed, the low-dose AAVrh10-cGALC-treated dogs had a reduced number of vector copies compared to the high-dose cohort (Table 2). Untreated normal dogs were used as controls.

AAVrh10 neutralizing antibody titers

Serum samples from all AAV-treated dogs and untreated controls were analyzed for the presence of neutralizing antibodies (NAbs) against AAVrh10. There was an absence of NAbs against AAVrh10 in untreated control dog serum samples at a limit of detection of 1:5. After i.v. injection but prior to ICV injection (around 45 days post i.v. injection), high-dose-treated dogs were seropositive for anti-AAVrh10 NAbs at a titer of 1:2,560 and 1:5,120. Interestingly, after ICV injection (60 days post i.v. injection), anti-AAVrh10 NAbs increased to 1:81,920 and 1:40,960. By 75 days post i.v. injection, NAbs for one of the high-dose-treated dogs decreased to 1:20,480 and further declined to 1:10,240 by 120 days post i.v. injection, where titers remained (assayed every 30 days) until the endpoint. For the other high-dose-treated dog, injection titers at 75 days post i.v. injection decreased to 1:10,240 and further declined to 1:5,120 by 90 days post i.v. injection, where they remained until the endpoint. At 90 days post i.v. injection, low-dose-treated dogs had titers of 1:5,120 and 1:10,240, respectively, and comparable titers were found in AAVrh10-GFP-treated dogs. As for the single dog treated with human GALC, anti-AAVrh10 NAbs after i.v. injection were 1:5,120 and increased to 1:81,920 after addition of the ICV injection (60 days post i.v. injection).

GFP biodistribution

Both dogs that received AAVrh10-GFP (Table 1) had a modest number of GFP-positive cortical neurons in the cerebrum (Fig. 3A and B) and GFP-positive Purkinje cells in the cerebellum (Fig. 3C and D) determined by cell size and morphology. Within the spinal cord, the single dog that received i.v. and ICV injection routes had a greater number of GFP-positive cells in the gray matter compared to the dog that received i.v. injection alone (Fig. 3E and F). Similarly, i.v. + ICV resulted in increased GFP expression in the dorsal root ganglion when compared to i.v. alone (Fig. 3G and H).

Histopathological evaluation of CNS

In untreated GLD dogs, there was near complete loss of myelination in the central cerebellar white matter, while the distal white matter of the folia retained some degree of myelin, as indicated by iron eriochrome (ECR) stain (Fig. 4B) and compared to a normal age-matched control dog (Fig. 4A). Accumulation of PAS-positive storage material, associated with infiltration of glycosphingolipid-laden macrophages, was seen in the cerebellar white matter of untreated GLD dogs (Fig. 4E) and was absent in normal age-matched control tissue (Fig. 4D). High-dose i.v. + ICV treatment with AAVrh10-cGALC resulted in near normal myeli-

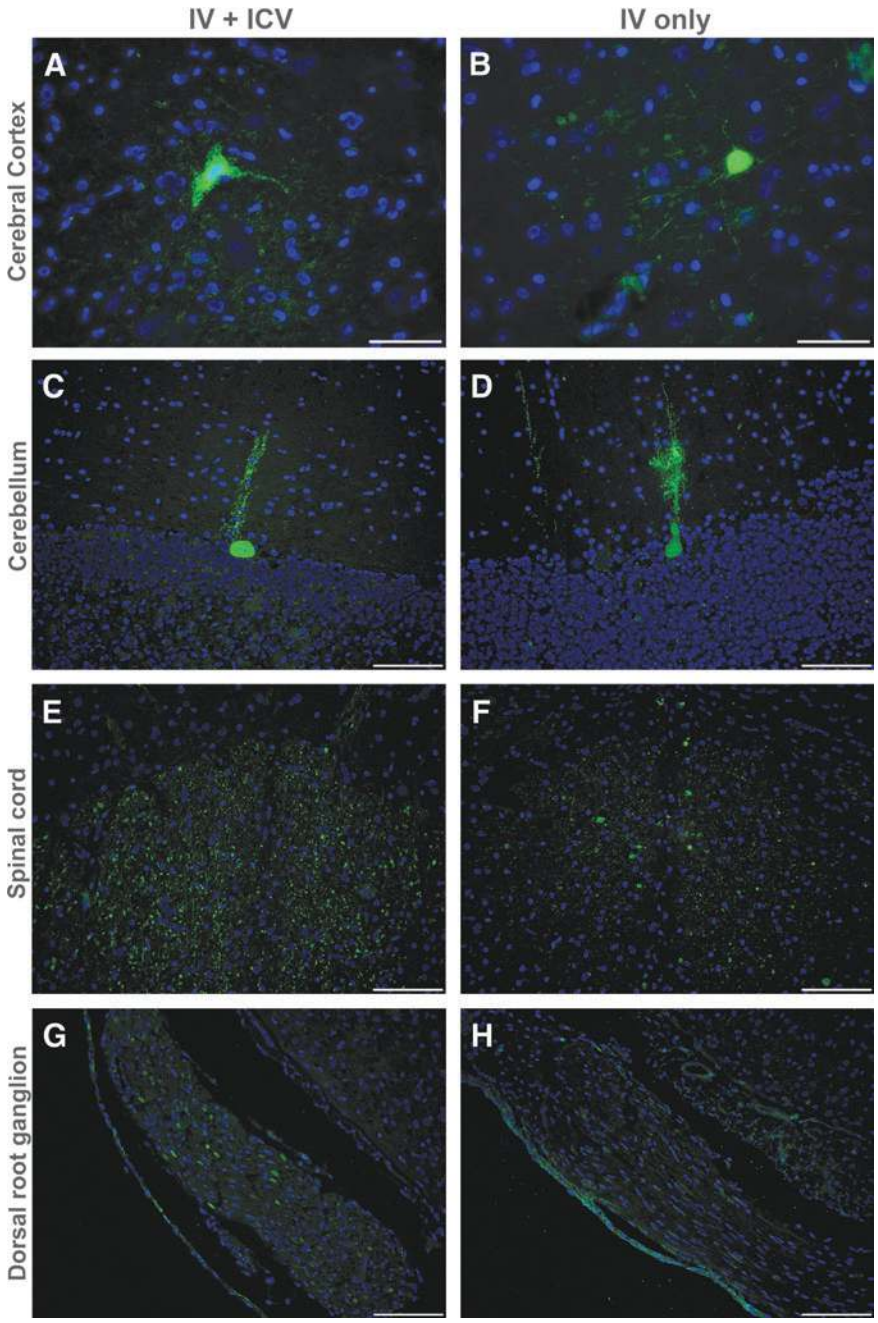

Figure 3. GFP Immunofluorescence in AAV-GFP-treated GLD dogs. GFP immunofluorescence staining in GLD dogs treated with AAVrh10 encoding GFP by intravenous (i.v.) and intracerebroventricular (ICV) or i.v. injection alone. Staining is shown in the cerebral cortex, cerebellum, spinal cord, and dorsal root ganglion for an i.v. + ICV-treated GLD dog **(A**, **C**, **E**, and **G)** and i.v. only treated dog **(B**, **D**, **F**, and **H)**. Bars in the lower right corner of images A and B = 50 μm and C–H = 100 μm.

nation (Fig. 4C) and reduction in storage product (Fig. 4F) in the cerebellum. There was a notable isolated area of white matter in the anterior lobe of the cerebellum and ventral pons that lacked myelination (Fig. 4C, arrows) and contained PAS-positive storage material (Fig. 4F, arrows).

Untreated GLD dogs demonstrated widespread microgliosis (indicated with increased Iba1 expression, red stain) and astrocytosis (indicated with increased GFAP expression, green stain; Fig. 4H) associated with areas of demyelination and accumulation of storage product compared to normal (Fig. 4G). High-dose i.v. + ICV treatment with AAVrh10-cGALC largely prevented the infiltration of microglia and astrocytes (Fig. 4I; region of interest [ROI] indicated by white box in Fig. 4C),

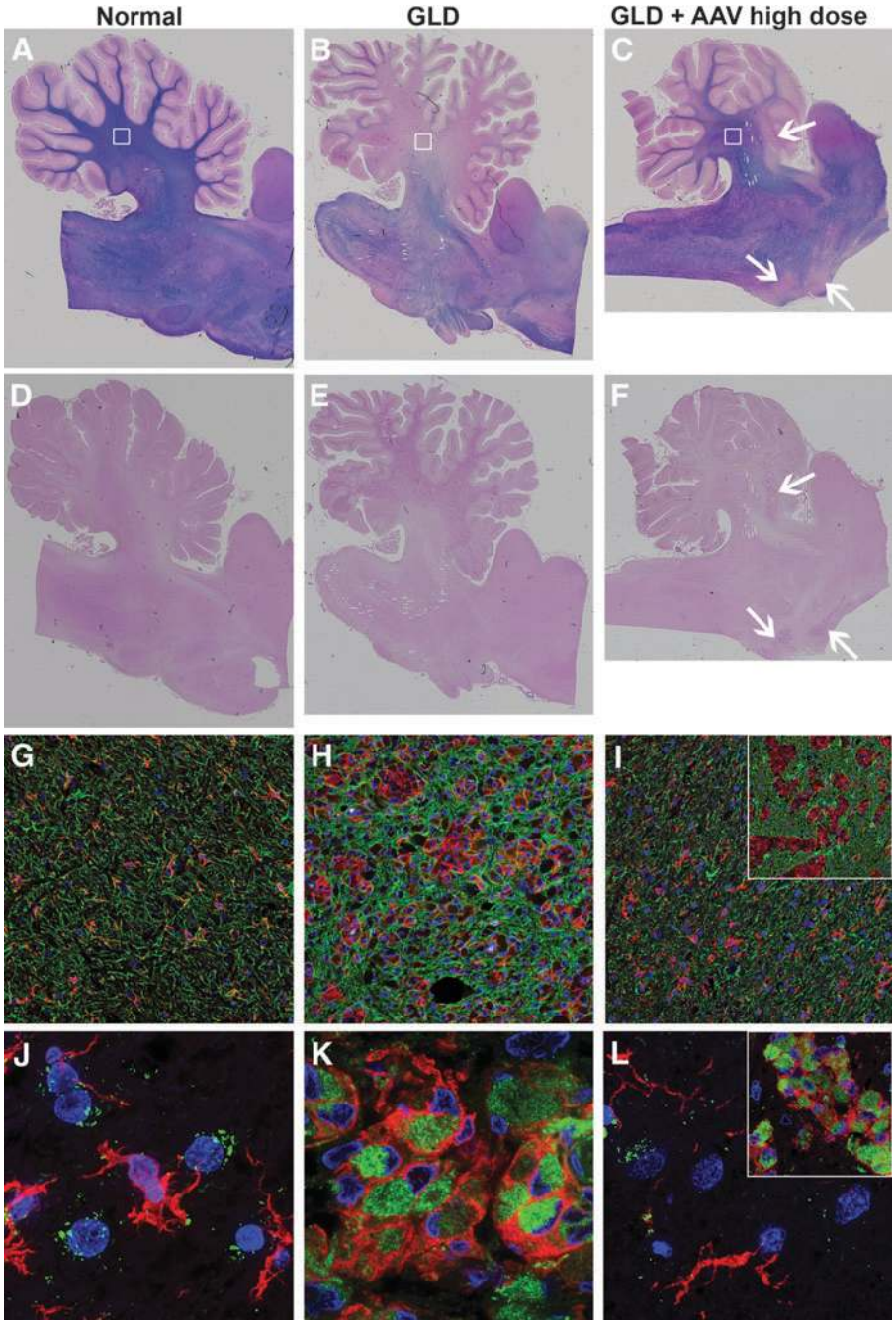

Figure 4. Histopathology in normal, GLD, and AAV-treated dogs. Iron eriochrome (ECR) stain specific for myelination shown in **(A)** normal, **(B)** GLD, and **(C)** high-dose AAV-treated dog at the level of the cerebellum. Periodic acid–Schiff (PAS) staining for polysaccharide detection in **(D)** normal, **(E)** GLD, and **(F)** high-dose AAV-treated dog. Iba1 (*red*) staining for microglia and GFAP (*green*) staining for astrocytes in **(G)** normal, **(H)** GLD, and **(I)** high-dose AAV-treated dogs. Region of image indicated by *white squares* in corresponding images **A–C**. Inset for **(I)** indicated by *white arrow* in anterior lobe of cerebellum. Iba1 (*red*) staining for microglia and LAMP1 (*green*) staining for lysosomal membranes in **(J)** normal, **(K)** GLD, and **(L)** high-dose AAV-treated dog. Region of image indicated by *white squares* in corresponding images **(A–C)**. Inset for L indicated by *white arrow* in anterior lobe of cerebellum.

except in the isolated areas of white matter that lacked myelination and contained PAS-positive storage material (Fig. 4I inset; ROI indicated by arrow in anterior lobe of cerebellum in Fig. 4C and F). In the untreated GLD dog, activated microglia (red) showed increased expression of LAMP1 (green), an indication of lysosomal expansion (Fig. 4K). In normal dogs, LAMP1 staining was mostly isolated within large neurons and not microglia (Fig. 4J). Gene therapy normalized LAMP1 expression (Fig. 4L; ROI indicated by white box in Fig. 4C), except in the isolated areas of white

matter in the anterior lobe of the cerebellum and ventral pons (Fig. 4L inset; ROI indicated by arrow in anterior lobe of cerebellum in Fig. 4C and F).

In the cerebrum, i.v. + ICV treatment with AAVrh10-cGALC failed to attenuate myelin loss fully or prevent storage accumulation (Supplementary Fig. S2). However, the high-dose cohort showed some modest improvement in myelination and storage over the low-dose cohort, especially in the longer-living dog (last column). In the spinal cord, i.v. + ICV treatment with AAVrh10-cGALC specifically failed to treat the lateral and ventral corticospinal tracts in the high-dose-treated dogs. In contrast to the cerebrum, the first dog of the low-dose cohort had the greatest level of correction in the spinal cord, while the second dog had diffuse loss of myelin and accumulation of storage in the white matter (Supplementary Fig. S3).

When analyzed by routine hematoxylin and eosin staining, the single dog treated with the human *GALC* transgene lacked infiltration of immune cells and necrosis, suggesting that there was not an acute immune reaction to the human protein. Additionally, the dog showed severe loss of myelination (ECR) and accumulation of storage material (PAS) comparable to untreated GLD dogs (data not shown).

Histopathological and morphometric analysis of PNS

Sections from the sciatic (mixed motor and sensory), tibial (mixed motor and sensory), and superficial radial (sensory) nerves from normal, untreated GLD, and AAVrh10-treated GLD dogs were evaluated. Compared to normal dogs, scattered nerve fibers from GLD-affected dogs showed inappropriately thin myelin sheaths for the axonal diameters (Fig. 5, 2nd row). Numerous acid phosphatase reactive macrophages (globoid cells) were apparent in GLD-affected dogs (Supplementary Fig. S4B) but not in normal age-matched control dogs (Supplementary Fig. S4A). Treatment with AAV-GFP did not reverse the histological changes (Fig. 5, 3rd row). In contrast, high-dose treatment with AAVrh10-GALC resulted in histologically improved myelin thickness (Fig. 5, 5th row) and loss of acid phosphatase reactive globoid cells in the frozen nerve sections (Supplementary Fig. S4C).

Axonal size frequency analysis was performed on the sciatic, tibial, and superficial radial nerves of treated GLD dogs, compared to normal and untreated nerves, and presented as a percentage of fibers $\leq 5\ \mu$m (small) and $>5\ \mu$m (large; Table 3). A shift toward a majority of small myelinated fibers ($\leq 5\ \mu$m) was apparent in the untreated GLD nerves, while in AAVrh10-GALC high-dose-treated GLD dogs, the ratio of small ($\leq 5\ \mu$m) and large ($>5\ \mu$m) fibers was normalized. For example, for the tibial nerve, GLD dogs had 87.84% and 96.27% of fibers $\leq 5\ \mu$m compared to normal dogs where only 57.92% and 69.14% of fibers were $\leq 5\ \mu$m. As expected, after combination gene therapy with AAVrh10-GFP, the frequency of axon size distribution was not improved (73.2% and 86.16% of fibers $\leq 5\ \mu$m). However, after treatment with high-dose AAVrh10-cGALC, the ratio of fiber size was normalized (53.76% and 66.65% of fibers $\leq 5\ \mu$m). The myelinated fiber density, thin myelin fiber density, and percentage of thinly myelinated fibers did not quantitatively differ among groups (Supplementary Table S1). Compared to untreated dogs, the average myelin thickness (Supplementary Table S2) showed a trend toward normal thickness in GLD dogs treated with high-dose AAVrh10-GALC therapy. This trend toward normal myelin thickness was consistent with the histological findings (Fig. 5).

DISCUSSION

Herein, the first AAV gene therapy experiments are presented in a canine model of GLD that closely recapitulates the clinical disease progression, neuropathological alterations, and biochemical abnormalities observed in human patients. Adapted from studies in twitcher mice, GLD dogs were treated by combination i.v. and ICV injections of AAVrh10 to target both PNS and CNS. Combination of i.v. and ICV AAV gene therapy had a clear dose response and resulted in delayed onset of clinical signs, extended life-span, correction of biochemical defects, and attenuation of neuropathology.

In mucopolysaccharidosis VII (MPSVII) dogs, it was previously shown that the addition of CNS-directed delivery of AAVrh10 by intrathecal injection increased the activity of the deficient enzyme, GUSB, in the brain and spinal cord when compared to i.v. injection alone.[27] This study, using AAVrh10 encoding *GFP*, evaluated if CNS-directed delivery of vector by ICV delivery via the lateral ventricle increased GFP expression when compared to i.v. injection alone. Both injection routes resulted in a modest number of GFP-positive cortical neurons and Purkinje cells. Notably, addition of ICV injection increased the number of GFP-positive cells in the gray matter of the spinal cord as well as dorsal root ganglion. Peripheral nerves from these animals were not available for immunohistochemistry, as they were preserved for electron microscopy and morphometry studies. Importantly, in contrast to the MPSVII study in which dogs received dif-

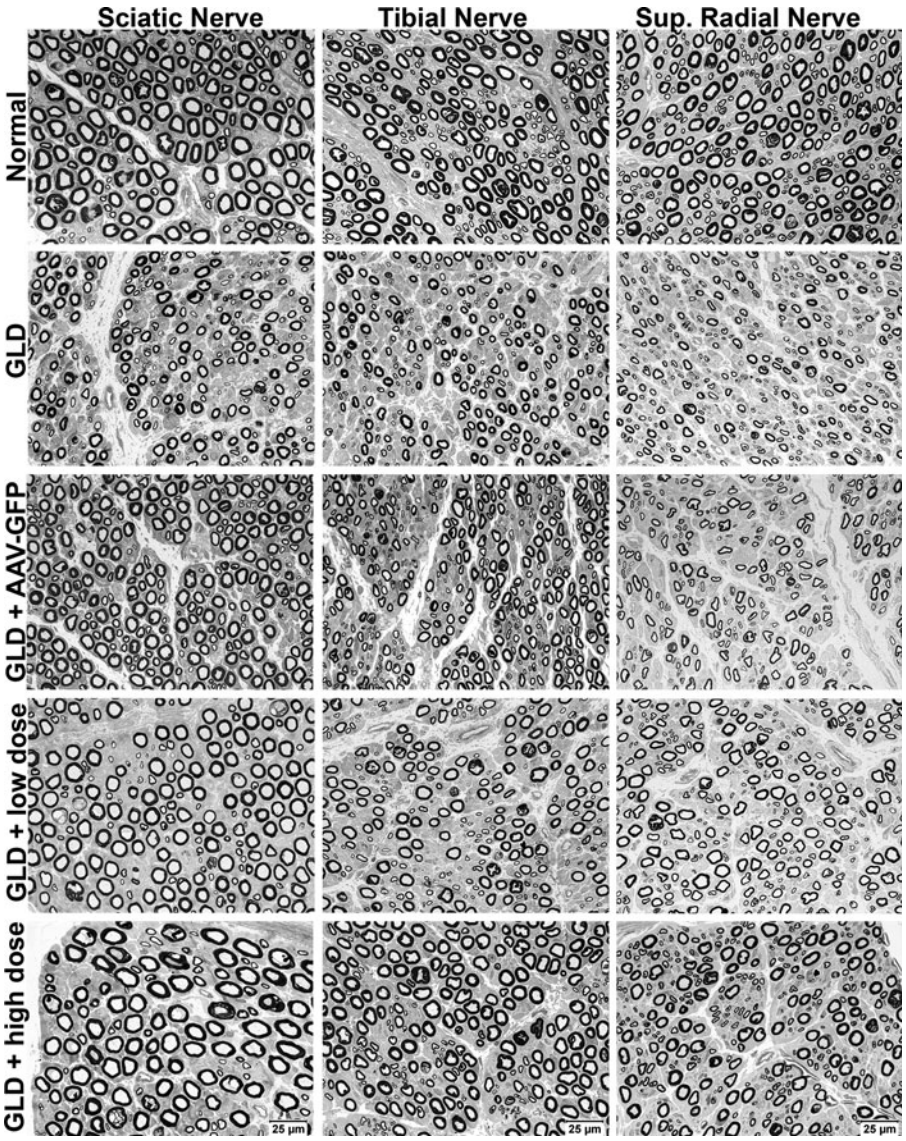

Figure 5. Peripheral nerve histopathology in normal, GLD, and AAV-treated dogs. Resin sections (1 μm) from the sciatic (mixed motor and sensory), tibial (mixed motor and sensory), and superficial radial (sensory) nerves of normal dogs (row 1), GLD (row 2), and AAV-treated dogs (rows 3–5) were evaluated using the paraphenelenediamine stain. Bars in lower-right corner of bottom-row images = 25 μm for all images.

Table 3. *Axonal size frequency distribution*

	Sciatic nerve		*Tibial nerve*		*Superficial radial nerve*	
	% Fibers ≤5 μm	*% Fibers >5 μm*	*% Fibers ≤5 μm*	*% Fibers >5 μm*	*% Fibers ≤5 μm*	*% Fibers >5 μm*
Normal	46.6	53.40	57.92	42.08	55.17	44.83
	78.97	21.03	69.14	30.86	55.56	44.44
GLD	55.87	44.13	87.84	12.16	76.17	23.83
	80.37	19.63	96.27	3.73	92.50	7.50
AAV-GFP	38.7	61.30	73.2	26.80	45.38	54.62
	64.48	35.52	86.16	13.84	70.06	29.94
AAV-cGALC low dose	44.9	55.10	53.98	46.02	45.95	54.05
	57.52	42.48	64.11	35.89	35.67	64.33
AAV-cGALC high dose	48.72	51.28	53.76	46.24	45.45	54.55
	60.3	39.70	66.56	33.44	56.73	43.27

Each row represents the percentage of fibers and sum to 100 for each of the three nerves: sciatic nerve, tibial nerve, and superficial radial nerve. Each column represents an individual dog.

GFP, green fluorescent protein.

ferent AAV serotypes (AAV9 and AAVrh10) for i.v. and intrathecal injections,[27] this study also proved the feasibility of combination systemic and CNS-directed delivery using the same AAV serotype.

It has previously been shown in studies evaluating AAV gene therapy in a canine model of MPSIIIA and a feline model of Sandhoff disease that the use of species-specific transgenes decreases immunogenicity and increases long-term transgene expression.[28,29] One GLD dog was treated with AAVrh10 expressing human GALC by i.v. and ICV delivery, and the dog showed no clinical benefit and died suddenly at 9 weeks of age. Postmortem evaluation showed no signs of acute inflammation of the brain, suggesting that there was not a detrimental immune reaction to the human protein. However, no therapeutic benefit was seen, although the dose was approximately three times greater than that in the low-dose AAVrh10-cGALC group and approximately 10 times less than that of the high-dose AAVrh10-cGALC group. The dog showed severe loss of myelin and accumulation of storage material comparable to untreated GLD dogs. Due to the unexpected death, endpoint electrodiagnostic testing was not conducted, and frozen tissues were not available for GALC and psychosine analysis to compare to the dogs detailed herein.

Additionally, four GLD dogs were treated with AAVrh10 expressing species-specific canine GALC. Combination i.v. and ICV delivery of AAVrh10-cGALC had a clear dose-dependent response. High-dose (3.8E13 vg) treated dogs had a greater delay in disease onset and lived longer when compared to low-dose (1.2E12 vg) treated dogs.

Notably, the GLD dogs treated with high dose i.v. and ICV AAVrh10-cGALC maintained normal nerve conduction velocities at the disease endpoint, signifying that correction of peripheral nerve disease after gene therapy was sufficient and also not transient. Despite correction of NCV, all AAVrh10-cGALC-treated dogs still developed pelvic limb spastic paralysis, suggesting that treatment of the CNS but not the PNS was the limitation of the therapy. Furthermore, neither low- nor high-dose-treated dogs showed improvement in central conduction time or hearing threshold, indicating that the therapy failed to correct auditory system abnormalities. This study on four dogs demonstrates that i.v. treatment at 3 days of age is capable of correcting the debilitating PNS disease associated with GLD, but ICV delivery at 6 weeks of age failed to correct CNS disease fully. This is important, since children affected with GLD who receive HSCT prior to the onset of symptoms, the current standard of care, show only transient improvement in NCV.[30]

In corroboration with NCV findings, high-dose-treated dogs showed improvement in myelin thickness and loss of acid phosphatase reactive globoid cells when compared to untreated and low-dose-treated dogs. Both low- and high-dose-treated dogs showed improvement in the ratio of small to large axons compared to untreated GLD dogs. Insufficient animal numbers made morphometric data difficult to interpret, as overlap in numerous parameters was seen between normal and untreated GLD dogs. Analysis of additional control animals is currently underway to define quantitative changes more clearly in peripheral nerves of GLD dogs.

In the CNS, high-dose-treated dogs showed greater improvement in demyelination, reduction in PAS-positive storage material, and attenuation of neuroinflammation (indicated by Iba1 and GFAP staining) and lysosomal accumulation (indicated by LAMP1 staining). Interestingly, the cerebellum showed greater improvement than did the cerebrum in both low- and high-dose cohorts. It is hypothesized that this could be due to the timing of myelination in the normal dog brain, as myelination of the cerebellum occurs <4 weeks of age, while myelination of the cerebrum is delayed until 4–16 weeks of age.[31] The two dogs from the high-dose cohort showed a similar pattern of spinal cord pathology, with lack of myelin and corresponding storage accumulation primarily limited to the lateral and ventral corticospinal tracts. These findings corroborate the pattern of correction in the brain, as the corticospinal tract is the last to myelinate in the spinal cord. These deficiencies in the cortical spinal tracts are consistent with the findings of spastic paralysis and are similar to the motor deficits present in children with GLD. However, in the low-dose cohort, the longer-living dog had near normal myelination and minimal storage accumulation in the spinal cord, while the shorter-living dog had widespread loss of myelin and marked accumulation of storage throughout the white matter and biochemically a higher concentration of psychosine.

Importantly, GLD dogs treated with the combination of i.v. and ICV AAV gene therapy still died of GLD-related disease, which remained in the CNS. Reasons for this include the possibilities that ICV therapy was provided too late in the disease course; too low a dose of AAV was administered; and/or ICV was an inefficient route of AAV administration. The authors have unpublished data demonstrating that psychosine is significantly elevated in the CSF of

GLD dogs by 4 weeks of age, suggesting that earlier targeting of the CNS may be necessary to treat GLD effectively. The impact of psychosine has previously been evaluated in rodent oligodendrocyte culture and oligodendrocyte precursor-like cell lines, and has been shown to impair differentiation and at specific concentrations result in cell death.[32,33] It is plausible that by 6 weeks of age, impaired maturation and/or death of oligodendrocytes in GLD dogs subsequently reduced the cellular targets for AAV-mediated GALC transduction, diminishing therapeutic efficacy in the CNS.

The inability to normalize psychosine levels despite complete restoration of GALC activity is an important finding for optimizing therapeutic outcomes. One plausible explanation is that psychosine accumulation was present at the time of treatment, and while further increase may have been attenuated, it was not reversed. Accumulated psychosine may also be located in non-lysosomal compartments or membranes and not capable of degradation by hydrolytic lysosomal GALC. It has previously been demonstrated that psychosine accumulates in lipid rafts in the brain and sciatic nerve of twitcher mice and in brain samples from human GLD patients.[34]

In addition to the psychosine issues, the extent of disease pathology in the brain of 6-week-old GLD dogs is unknown. If substantial disease pathology is already present, this may limit the efficacy of therapy provided at this point in time. Second, only the high dose of AAVrh10 proved effective in ameliorating CNS disease in the GLD dog. A higher concentration may have proven to be in more effective. Finally, there is some evidence that intrathecal AAV administration results in different patterns of gene expression, depending on whether it is given ICV, at the cerebellmedullary cistern, or lumbar cistern.[35] Earlier treatment of the CNS can be achieved by replacing ICV injections with less invasive cerebellomedullary cistern injections, which are now being explored.

Biochemically, the high-dose-treated dogs achieved normalized levels of GALC activity in the brain, spinal cord, sciatic nerve, and liver. Not all tissues were available for analysis for the low-dose cohort. However, GALC activity was below the level of detection in the spinal cord and sciatic nerve and only modestly increased in the liver of low-dose-treated dogs. The cerebellum and sciatic nerve proved to have the highest level of psychosine accumulation in untreated GLD dogs. Notably, in the cerebellum, one high-dose-treated dog had greater than normal GALC activity. Yet, psychosine concentration was still seven times normal levels. The longer-living high-dose-treated dog achieved GALC activity in the cerebellum that was seven times that found in normal dogs, with correspondingly higher vector copies, and psychosine concentration was reduced to near normal levels. The longer-living high-dose-treated dog also had lower psychosine levels in the cerebrum, spinal cord, and liver. These results emphasize the importance of not relying solely on restoration of GALC enzyme activity as a therapeutic readout, as psychosine concentration may serve as a more functional indication of treatment efficacy.

It has been previously shown that psychosine is significantly elevated in the CSF of untreated GLD dogs compared to normal age-matched controls.[18] Here, it has been demonstrated that high-dose-treated dogs resulted in a greater reduction in CSF psychosine levels when compared to low-dose-treated and untreated GLD dogs, suggesting this as a plausible biomarker of disease progression and therapeutic efficacy. Psychosine levels after low-dose AAV were higher than in untreated GLD samples. This is believed to be due to the advanced age of the low-dose-treated animals (21 and 18 weeks of age) compared to the untreated GLD dogs, which averaged 13.4 weeks of age. CSF samples for this analysis were collected without the addition of a detergent recently shown to reduce the loss of lipid (data not shown). Therefore, it is expected that values of CSF psychosine in all cohorts are underrepresented here. Longitudinal analysis of psychosine levels in serum, plasma, and CSF of untreated GLD dogs is ongoing.

It is plausible that expression of the therapeutic transgene from the ICV injection was compromised by circulating Nabs to the AAVrh10 capsid and/or *GALC* transgene due to prior exposure from the systemic injection. After i.v. injection but prior to ICV injection, high-dose-treated dogs were seropositive for anti-AAVrh10 NAbs at titers of 1:2,560 and 1:5,120. After ICV injection with the same capsid, anti-AAVrh10 NAbs increased to 1:81,920 and 1:40,960. A large number of vector copies (>1E + 06) were present at the endpoint in the brain, spinal cord, and liver, indicating that despite high circulating antibody titers to the capsid, the humoral immune response did not eliminate long-term vector presence. Normal levels of GALC activity were achieved in the brain, spinal cord, sciatic nerve, and liver of high-dose-treated dogs, which is not suggestive of a detrimental immune response against the therapeutic protein. Due to limited CSF volume from treated dogs, neutralizing antibodies were not assessed in the CSF. Purified canine GALC enzyme or peptide library were

not available to serve as antigens to determine if an immune response was present to the therapeutic protein or if the i.v. dose was sufficient to tolerize animals. In the aforementioned study, MPSVII dogs received an i.v. injection at 3 days of age with AAV9 or AAVrh10 followed by intrathecal injection at 2 months of age with the opposite serotype. Prior i.v. delivery did not compromise distribution of the intrathecal delivered vector when a different serotype was used.[27] This study demonstrates for the first time feasibility of using the same vector capsid for both systemic and CNS-directed injections in dogs.

The data provided above will be used to direct future studies, including (1) evaluating the efficacy of i.v. therapy alone on treating the PNS in GLD dogs, and (2) studying how higher vector doses, alternate CNS-directed injection routes, and earlier intervention effect the treatment of CNS aspects of the disease. Finally, it was previously demonstrated that AAVrh10 provides strong neuronal transduction in the canine brain. However, this serotype failed to transduce glia or oligodendrocytes.[36] It is probable that targeting specific cell types, namely oligodendrocytes, may also improve disease outcome.

Most recently, HSCT in combination with AAV gene therapy has been evaluated in the twitcher mouse, and dramatic results were shown.[37] These studies are currently being adapted for the GLD dog and are ongoing. HSCT was attempted in a single GLD dog ~20 years ago following whole-body radiation, which confounded demyelination pathology.[19] In contrast, ongoing studies in twitcher mice and GLD dogs utilize a clinically relevant chemical ablation protocol. The effects of HSCT alone and HSCT in combination with AAV gene therapy will be compared to the GLD dogs treated herein to help determine the best clinical course for treatment of GLD.

CONCLUSION

For the first time, therapeutic effect in the canine model of GLD has been established by targeting both the PNS and CNS. Combination i.v. and ICV AAV gene therapy had a clear dose-dependent response, was capable of more than doubling the life-span of GLD dogs, and largely corrected PNS defects. These studies provide clear direction in optimization of dose and CNS-directed delivery, which are ongoing. It is believed that strong preclinical data in this highly translatable model will provide a direct route to clinical implementation and improve the treatment outcomes for children with GLD.

ACKNOWLEDGMENTS

This study was partially funded by The Legacy of Angels (D.A.W.), NIH OD P40-10939 (C.H.V.), NIH R01 NS096087 (C.H.V), NIH R01 NS065808 (E.R.B), and Jay Goldman Stewardship (A.M.B.). M.S.M. is funded through a NRSA fellowship (F30NS090684); A.M.B. is funded through a NRSA fellowship (F32NS093898). We thank Zane Hauck and Richard van Breemen (UIC-RRC) for assistance with psychosine determination and students at the University of Pennsylvania School of Veterinary Medicine for animal care. We would also like to acknowledge the Krabbe Translational Research Network.

AUTHOR DISCLOSURE

No competing financial interests exist.

REFERENCES

1. Duffner PK, Jalal K, Carter RL. The Hunter's Hope Krabbe family database. Pediatr Neurol 2009;40: 13–18.
2. Duffner PK, Barczykowski A, Jalal K, et al. Early infantile Krabbe disease: results of the World-Wide Krabbe Registry. Pediatr Neurol 2011;45: 141–148.
3. Escolar ML, Poe MD, Provenzale JM, et al. Transplantation of umbilical-cord blood in babies with infantile Krabbe's disease. N Engl J Med 2005;352:2069–2081.
4. Aldenhoven M, Kurtzberg J. Cord blood is the optimal graft source for the treatment of pediatric patients with lysosomal storage diseases: clinical outcomes and future directions. Cytotherapy 2015; 17:765–774.
5. Hoogerbrugge PM, Poorthuis BJ, Romme AE, et al. Effect of bone marrow transplantation on enzyme levels and clinical course in the neurologically affected twitcher mouse. J Clin Invest 1988;81:1790–1794.
6. Yeager AM, Brennan S, Tiffany C, et al. Prolonged survival and remyelination after hematopoietic cell transplantation in the twitcher mouse. Science 1984;225:1052–1054.
7. Yeager AM, Shinohara M, Shinn C. Hematopoietic cell transplantation after administration of high-dose busulfan in murine globoid cell leukodystrophy (the twitcher mouse). Pediatr Res 1991;29: 302–305.
8. Kondo A, Hoogerbrugge PM, Suzuki K, et al. Pathology of the peripheral nerve in the twitcher mouse following bone marrow transplantation. Brain Res 1988;460:178–183.

9. Ricca A, Rufo N, Ungari S, et al. Combined gene/cell therapies provide long-term and pervasive rescue of multiple pathological symptoms in a murine model of globoid cell leukodystrophy. Hum Mol Genet 2015;24:3372–3389.
10. Li YD, Sands MS. Experimental therapies in the murine model of globoid cell leukodystrophy. Pediatr Neurol 2014;51:600–606.
11. Rafi MA, Zhi Rao H, Passini MA, et al. AAV-mediated expression of galactocerebrosidase in brain results in attenuated symptoms and extended life span in murine models of globoid cell leukodystrophy. Mol Ther 2005;11:734–744.
12. Lin DS, Hsiao CD, Liau I, et al. CNS-targeted AAV5 gene transfer results in global dispersal of vector and prevention of morphological and function deterioration in CNS of globoid cell leukodystrophy mouse model. Mol Genet Metab 2011;103:367–377.
13. Reddy AS, Kim JH, Hawkins-Salsbury JA, et al. Bone narrow transplantation augments the effect of brain- and spinal cord-directed adeno-associated virus 2/5 gene therapy by altering inflammation in the murine model of globoid-cell leukodystrophy. J Neurosci 2011;31:9945–9957.
14. Rafi MA, Rao HZ, Luzi P, et al. Extended normal life after AAVrh10-mediated gene therapy in the mouse model of Krabbe disease. Mol Ther 2012;20:2031–2042.
15. Wenger DA, Victoria T, Rafi MA, et al. Globoid cell leukodystrophy in cairn and West Highland white terriers. J Hered 1999;90:138–142.
16. Victoria T, Rafi MA, Wenger DA. Cloning of the canine GALC cDNA and identification of the mutation causing globoid cell leukodystrophy in West Highland White and Cairn terriers. Genomics 1996;33:457–462.
17. Fletcher TF, Kurtz HJ, Low DG. Globoid cell leukodystrophy (Krabbe type) in the dog. J Am Vet Med Assoc 1966;149:165–172.
18. Bradbury AM, Bagel JH, Jiang X, et al. Clinical, electrophysiological, and biochemical markers of peripheral and central nervous system disease in canine globoid cell leukodystrophy (Krabbe's disease). J Neurosci Res 2016;94:1007–1017.
19. McGowan JC, Haskins M, Wenger DA, et al. Investigating demyelination in the brain in a canine model of globoid cell leukodystrophy (Krabbe disease) using magnetization transfer contrast: preliminary results. J Comp Assist Tomogr 2000;24:316–321.
20. Vite CH, Cross JR. Correlating magnetic resonance findings with neuropathology and clinical signs in dogs and cats. Vet Radiol Ultrasound 2011;52:S23–31.
21. Bradbury A, Peterson D, Vite C, et al. Diffusion tensor imaging analysis of the brain in the canine model of Krabbe disease. Neuroradiol J 2016;29:417–424.
22. Gao G, Vandenberghe LH, Alvira MR, et al. Clades of adeno-associated viruses are widely disseminated in human tissues. J Virol 2004;78:6381–6388.
23. Lock M, Alvira M, Vandenberghe LH, et al. Rapid, simple, and versatile manufacturing of recombinant adeno-associated viral vectors at scale. Hum Gene Ther 2010;21:1259–1271.
24. Calcedo R, Vandenberghe LH, Gao G, et al. Worldwide epidemiology of neutralizing antibodies to adeno-associated viruses. J Infect Dis 2009;199:381–390.
25. Mizisin AP, Kalichman MW, Bache M, et al. NT-3 attenuates functional and structural disorders in sensory nerves of galactose-fed rats. J Neuropathol Exp Neurol 1998;57:803–813.
26. Mizisin AP, Shelton GD, Burgers ML, et al. Neurological complications associated with spontaneously occurring feline diabetes mellitus. J Neuropathol Exp Neurol 2002;61:872–884.
27. Gurda BL, De Guilhem De Lataillade A, Bell P, et al. Evaluation of AAV-mediated gene therapy for central nervous system disease in canine mucopolysaccharidosis VII. Mol Ther 2016;24:206–216.
28. Haurigot V, Marco S, Ribera A, et al. Whole body correction of mucopolysaccharidosis IIIA by intracerebrospinal fluid gene therapy. J Clin Invest 2013 Jul 1 [Epub ahead of print]; DOI: 10.1172/JCI66778.
29. Bradbury AM, Cochran JN, McCurdy VJ, et al. Therapeutic response in feline sandhoff disease despite immunity to intracranial gene therapy. Mol Ther 2013;21:1306–1315.
30. Siddiqi ZA, Sanders DB, Massey JM. Peripheral neuropathy in Krabbe disease: effect of hematopoietic stem cell transplantation. Neurology 2006;67:268–272.
31. Gross B, Garcia-Tapia D, Riedesel E, et al. Normal canine brain maturation at magnetic resonance imaging. Vet Radiol Ultrasound 2010;51:361–373.
32. Cho KH, Kim MW, Kim SU. Tissue culture model of Krabbe's disease: psychosine cytotoxicity in rat oligodendrocyte culture. Dev Neurosci 1997;19:321–327.
33. Won JS, Kim J, Paintlia MK, et al. Role of endogenous psychosine accumulation in oligodendrocyte differentiation and survival: implication for Krabbe disease. Brain Res 2013;1508:44–52.
34. White AB, Givogri MI, Lopez-Rosas A, et al. Psychosine accumulates in membrane microdomains in the brain of krabbe patients, disrupting the raft architecture. J Neurosci 2009;29:6068–6077.
35. Hinderer C, Bell P, Katz N, et al. Evaluation of intrathecal routes of administration for adeno-associated viral vectors in large animals. Hum Gene Ther 2018;29:15–24.
36. Swain GP, Prociuk M, Bagel JH, et al. Adeno-associated virus serotypes 9 and rh10 mediate strong neuronal transduction of the dog brain. Gene Ther 2014;21:28–36.
37. Rafi MA, Rao HZ, Luzi P, et al. Long-term improvements in lifespan and pathology in CNS and PNS after BMT plus one intravenous injection of AAVrh10-GALC in twitcher mice. Mol Ther 2015;23:1681–1690.

Received for publication August 9, 2017;
accepted after revision January 7, 2018.

Published online: January 9, 2018.